18.1 A Self-Health-Learning GaN Power Converter Using On-Die Logarithm-Based Analog SGD Supervised Learning and Online T_J-Independent Precursor Measurement

Yuanqing Huang, Yingping Chen, D. Brian Ma

The University of Texas at Dallas, Richardson, TX

As GaN technology proliferates in modern power electronics, reliability of GaN-based circuits has become the biggest hurdle for commercialization. Sustaining largest voltage and current stresses in power circuits, power devices on average account for over 31% of failures [1]. With new problems such as current collapse and thermal aging, GaN power circuits deem to face more reliability challenges compared to their silicon counterparts [2]. In such a situation, health condition monitoring is of paramount importance. As shown in Fig. 18.1.1, due to hot electron injection and charge trapping effects, current collapse weakens 2-dimensional electron gas (2DEG) layer in a GaN switch over time, elevating its dynamic on-resistance r_{DS_ON} gradually. The clear link between r_{DS_ON} and aging (Fig. 18.1.1) makes r_{DS_ON} a widely accepted precursor for GaN condition monitoring [3-5]. However, measuring r_{DS_ON} is not a simple task. Traditionally, r_{DS_ON} can be measured offline by shutting down the affiliated circuit. However, the approach can be highly inaccurate due to significant discrepancy between offline and online operation conditions. To mitigate this issue, in-situ condition monitoring can be employed [3, 4]. However, it still requires designated test periods, causing interruptions of operation and increased test cost. A recent study applies machine learning (ML) to achieve online aging prognosis [5]. However, the ML algorithm is generic and is built on a standard digital basis. It requires sophisticated data processing and communication modules, causing substantial power and cost overheads. More importantly, the off-board look-up-table-based training process has to be performed offline, leading to similar drawbacks encountered in other approaches. Overall, all approaches reviewed here demand significant resources and time for either trimming, calibration or training in order to compensate for variations and errors induced by the fabrication process, work condition, user influence, etc. It would be much more desirable and efficient if a "plug-and-play" online aging prognosis method can be developed, which, as an essential part of a power circuit, requires no trimming and calibration.

To achieve the above goal, this paper presents a self-health-learning smart power converter in Fig. 18.1.2 and demonstrates two key design efforts. First, we present an on-die logarithm-based supervised learning engine for power device health prognosis. By taking advantage of sense/control signals available in the controller of the power converter, the engine autonomously trains the converter to establish and update its own r_{DS_ON} aging model without interrupting normal operation. As an integral part of the converter, the engine is designed using low-power, low-cost analog trans-linear circuits with no analog-to-digital data conversion. Compared to the off-chip FPGA-based ML approach proposed in [5], it computes much faster and more efficiently with minimized cost and power overhead. Second, we present a junction temperature (T_J) independent precursor measurement scheme for online condition monitoring. As r_{DS_ON} is highly T_J-dependent, the accuracy of aging prognosis heavily relies on effective removal of temperature impact from the r_{DS_ON} obtained in the 1st effort. Unlike conventional T_J sensing approaches, the proposed scheme eliminates the needs of direct parameter sensing on a GaN device, achieving a truly non-intrusive operation. To achieve it, the scheme computes instant power losses and sense ambient temperature T_A to determine the instant T_J.

Figure 18.1.3 details the proposed logarithm-based analog stochastic gradient descent (SGD) supervised learning algorithm. By collecting online sense/control signals (V_O, I_O, V_{IN}) as well as T_A and r_{DS_ON}, the converter starts the 1st step of training phase for data collection and power loss (P_{LOSS}) extraction. P_{LOSS} is extracted by evaluating conduction loss (P_{ON}), switching loss (P_{SW}) and output capacitance loss (P_{COSS}). T_J is then determined by $T_J=W_0+W_1\times T_A+W_2\times P_{COSS}+W_3\times P_{SW}+W_4\times P_{ON}$. Here, $W_{0\text{-}4}$ are the weights which are continuously updated in training process. Note that, due to the parasitics in the actual implementation, P_{LOSS} in practice is usually different from that of its theoretical calculation. Thus, to improve the model accuracy, a constant term W_0 is added to minimize the errors. In the 2nd step, r_{DS_ON} is predicted based on an exponential functionality inspired by the device physics indicating that $r_{DS\_ON}=\exp(a\times T_J+b)$. Here, a and b are technology related coefficients. Computing exponentials is usually resource-demanding in terms of circuit implementation. To mitigate this, a natural logarithm operation is applied to the above equation, transforming the equation to a linear function $\mathrm{Ln}(r_{DS\_ON})=a\times T_J+b$. With this transformation, the computation in SGD algorithm is fully linearized, significantly simplifying the complexity of data processing. In the circuit implementation, a BJT transconductance-based logarithmic converter is employed to efficiently complete the natural logarithmic operator. Using this relation, the on-resistance is predicted as r_{DS_ON}', which is then compared to the sensed r_{DS_ON}. The resulting difference is squared to generate the loss function L in the 3rd step. The weight's gradient is computed using the partial derivative of L with respect to each weight during the 4th step. Thanks to the linearization through the logarithm operation, the gradient computing is down-graded to first order partial differential, simplifying the circuits design. The gradients are then multiplied by a learning rate α. The results are subtracted from the previous $W_{0\text{-}4}$, generating the new weights in the 5th step. At last, the new weights are updated into local memory unit. Such iteration repeats every 64 clocks to minimize the L. Eventually, r_{DS_ON}' converges to r_{DS_ON}. In prediction phase, the predicted r_{DS_ON}' is used as an adaptive aging reference for T_J-independent online aging prognosis.

Figure 18.1.4 shows the circuit implementation of the T_J-independent online condition monitoring. To obtain r_{DS_ON}, the drain-source voltage V_{DS_ON} and current I_{DS_ON} of the high-side GaN switch M_T are measured. Then they are fed into an analog divider based on translinear principle. The translinear loop, consisting of Q_{N1}-Q_{N4}, achieves $I_{OUT}=I_{LSB}\times(I_{IN}/I_{IN2})$. Here, I_{LSB} is a unit current of the computation. As mentioned earlier, r_{DS_ON} varies with T_J fluctuations, degrading the condition monitoring accuracy. To remove T_J influence on r_{DS_ON}, T_J sensing is necessary. To achieve non-intrusive operation, an online T_J sensing scheme is proposed by evaluating T_A and P_{LOSS}. As detailed in Fig. 18.1.4, in addition to V_{IN} and V_O, I_{DS_ON} is fed to an averaging block. Controlled by the on-time of the converter, I_{DS_ON} is averaged to obtain I_O. To detect T_A, a proportional-to-absolute-temperature (PTAT) based voltage reference is designed. The circuit generates a PTAT voltage V_{PTAT} with a temperature coefficient of 1.793mV/°C. To avoid self-heating effect, the T_A sensor is placed away from the gate driver in the chip floorplan. The designed V_{PTAT} versus I_O data shows a near-constant V_{PTAT} when I_O varies from 0 to 1.8A, demonstrating high immunity to self-heating.

A prototype of this work is fabricated in a 0.18μm HV BCD process. Two enhancement-mode GaN FETs are used as power switches M_T and M_B. The converter supports the operation of V_{IN} from 5 to 40V, delivering 9W of power at switching frequency of 3.3MHz. To validate the training engine, 120 groups of raw data, including the power and ambient temperature parameters, are collected. As shown in Fig. 18.1.5, the proposed training engine delivers a model as $\mathrm{Ln}(r_{DS\_ON})=0.0043\times T_J+4.9$. Compared to the model provided by the manufacturer, which is $\mathrm{Ln}(r_{DS\_ON})=0.0036\times T_J+5.01$, the errors of temperature coefficient and constant term are 19.4% and -0.8%, respectively. Within the temperature range from 0°C to 120°C, the two errors compensate each other, ensuring the prediction accuracy. To verify the prediction accuracy, the trained model is applied to a group of measured data, showing the maximum prediction error of 2.77%. This resolution well suffices for condition monitoring. The inset of Fig. 18.1.5 shows the measured results on multiplication, demonstrating a linear increase of output O when input A varies from 0 to 0.9. The multiplier has a constant offset of 0.718, which is independent of the inputs. Thus, it can be easily removed from the output O through software algorithm. Figure 18.1.6 shows the measured V_{PTAT} increasing with T_A at a rate of 1.798mV/°C, matching the simulated value precisely. The measured r_{DS_ON}-T_J data verifies the exponential functionality. V_{DS_ON} increases from 160mV to 220mV when T_J rises from 25°C to 110°C. Fig. 18.1.7 shows the chip micrograph. The chip has an active area of 2.9mm^2.

Acknowledgement:
This work is in part sponsored by National Science Foundation (NSF) under the research contract NSF CCF 1702496.

References:

[1] H. Oh et al., "Physics-of-Failure, Condition Monitoring, and Prognostics of Insulated Gate Bipolar Transistor Modules: A Review," *IEEE Trans. Power Electronics*, vol. 30, no. 5, pp. 2413-2426, May 2015.

[2] S.R. Bahl et al., "Application Reliability Validation of GaN Power Devices," *IEDM*, pp. 544-547, Dec. 2016.

[3] J. Liu et al., "*In situ* Condition Monitoring of IGBTs Based on the Miller Plateau Duration," *IEEE Trans. Power Electronics*, vol. 34, no. 1, pp. 769-782, Jan. 2019.

[4] Y. Chen and D.B. Ma, "A 10MHz i-Collapse Failure Self-Prognostic GaN Power Converter with T_J-Independent In-Situ Condition Monitoring and Proactive Temperature Frequency Scaling," *ISSCC*, pp. 249–250, Feb. 2019.

[5] M. Biglarbegian et al., "On Condition Monitoring of High Frequency Power GaN Converters with Adaptive Prognostics," *IEEE Applied Power Electronics Conference and Exposition (APEC)*, pp. 1272-1279, Mar. 2018.

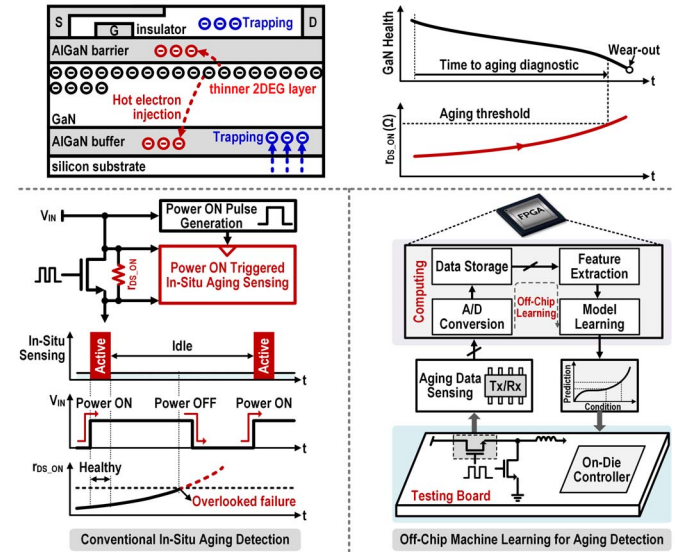

Figure 18.1.1: Challenges of condition monitoring for GaN power devices.

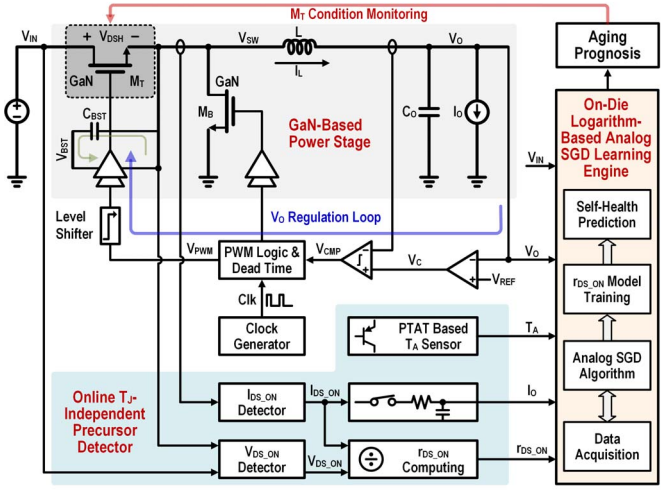

Figure 18.1.2: Illustration of a GaN power converter integrated with proposed logarithm-based analog SGD learning engine and online T_J-independent precursor measurement.

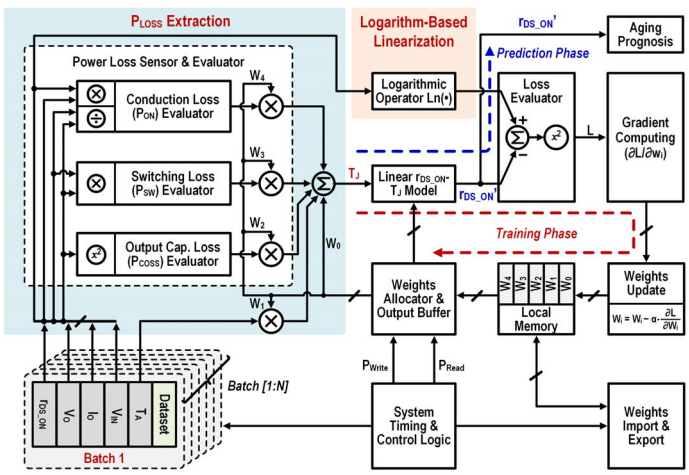

Figure 18.1.3: Online supervised learning using logarithm-based analog stochastic gradient descent (SGD) training algorithm for GaN device self-health-learning.

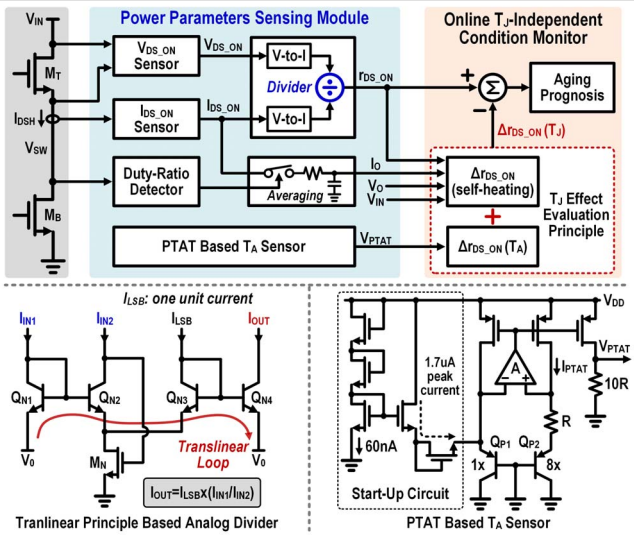

Figure 18.1.4: Circuit implementation of T_J-independent online condition monitoring with on-chip sensing blocks.

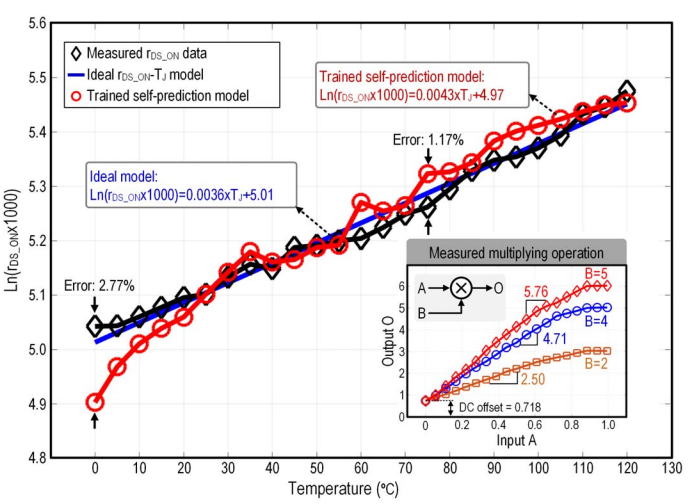

Figure 18.1.5: Measured results of the on-die supervised learning for r_{DS_ON}-temperature model training.

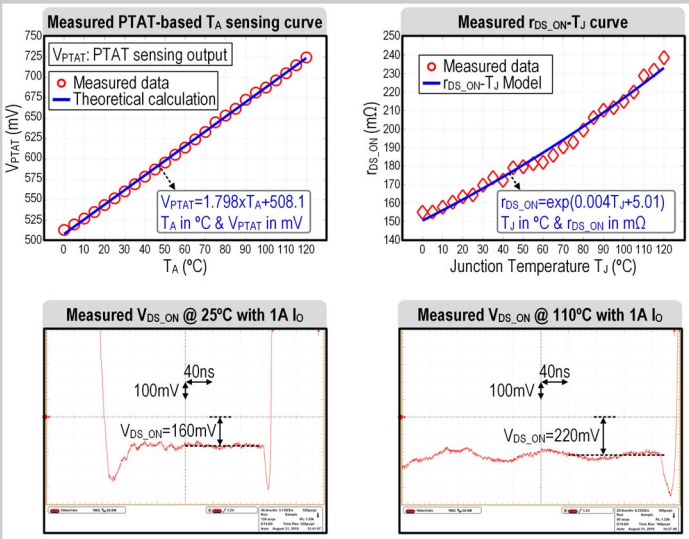

Figure 18.1.6: Measured results of the PTAT-based T_A sensing and temperature performance of the r_{DS_ON}.

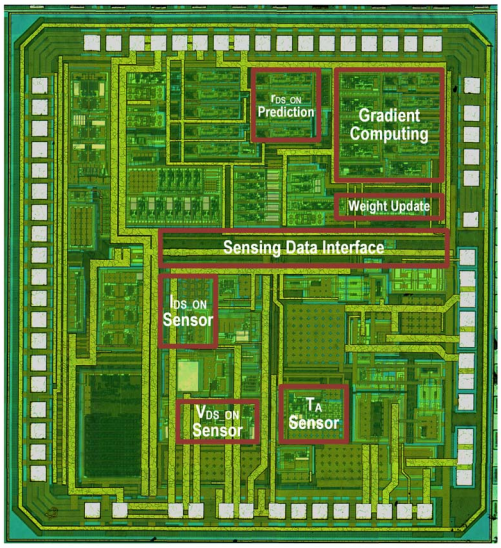

Figure 18.1.7: Chip micrograph.

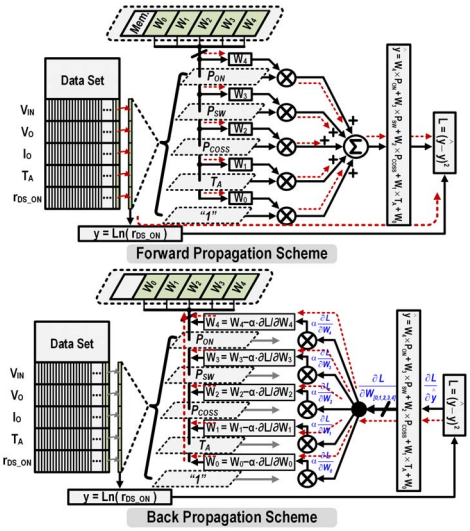

Figure 18.1.S1: Illustration of forward and back propagation schemes in online supervised learning.

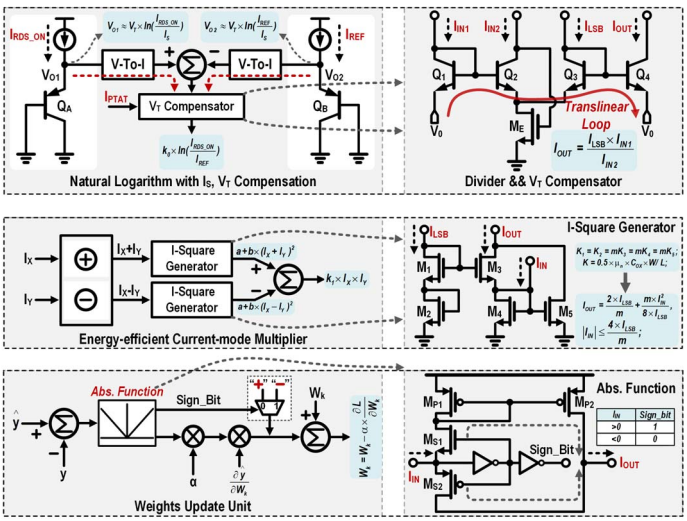

Figure 18.1.S2: Circuit implementations of analog natural logarithm, multiplier and weights update unit.

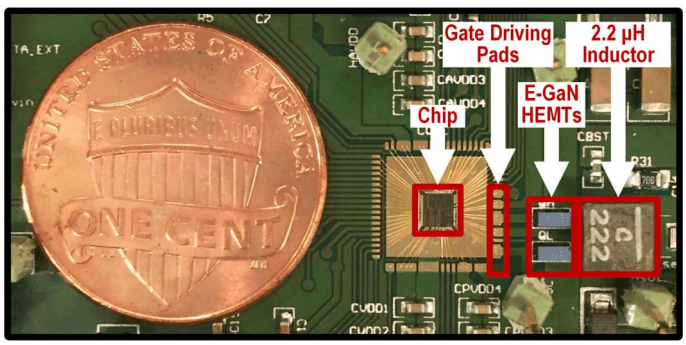

Figure 18.1.S3: Photo of the test board.

978-1-7281-3205-1/20/$31.00 ©2020 IEEE